J Mol Model (2013) 19:5611–5624
DOI 10.1007/s00894-013-2048-9

ORIGINAL PAPER

Molecular interactions of alcohols with zeolite BEA and MOR frameworks

Kai Stückenschneider · Juliane Merz · Gerhard Schembecker

Received: 2 September 2013 / Accepted: 21 October 2013 / Published online: 24 November 2013

Abstract Zeolites can adsorb small organic molecules such as alcohols from a fermentation broth. Also in the zeolite-catalyzed conversion of alcohols to biofuels, biochemicals, or gasoline, adsorption is the first step. Several studies have investigated the adsorption of alcohols in different zeolites experimentally, but computational investigations in this field have mostly been restricted to zeolite MFI. In this study, the adsorption of C1–C4 alcohols in BEA and MOR was investigated using density functional theory (DFT). Calculated adsorption geometries and the corresponding energies of the designed cluster models were comparable to periodic calculations, and the adsorption energies were in the same range as the corresponding computational and experimental values reported in the literature for zeolite MFI. Thus, BEA and MOR may be good adsorption materials for alcohols in the field of downstream processing and catalysis. Aside from the DFT calculations, adsorption isotherms were determined experimentally in this study from aqueous solutions. For BEA, the adsorption of significant amounts of alcohol from aqueous solution was observed experimentally. In contrast, MOR was loaded with only a very small amount of alcohol. Although differences were found between the affinities obtained from gas-phase DFT calculations and those observed experimentally in aqueous solution, the computational data presented here represent molecular level information on the geometries and energies of C1–C4 alcohols adsorbed in zeolites BEA and MOR. This knowledge should prove very useful in the design of zeolite materials intended for use in adsorption and catalytic processes, as it allows adsorption behavior to be predicted via judiciously designed computational models.

Keywords Adsorption · Alcohols · BEA · Density functional theory · MOR · Zeolites

Electronic supplementary material The online version of this article (doi:10.1007/s00894-013-2048-9) contains supplementary material, which is available to authorized users.

K. Stückenschneider · J. Merz (✉) · G. Schembecker
Laboratory of Plant and Process Design, Department of Biochemical and Chemical Engineering, TU Dortmund University, 44227 Dortmund, Germany
e-mail: juliane.merz@bci.tu-dortmund.de

Introduction

The fermentative production of biofuels such as bioethanol and biobutanol has drawn increasing attention over the last decade due to the rise in the amount of biofuel produced globally, economic interest in biofuels, and their importance. One example of a biofuel production process is the ABE process, where acetone–butanol–ethanol is produced by fermentation [1–6]. In such processes, the alcohol is often recovered through distillation, which is a relatively energy-consuming operation and cannot always be used. For instance, in the ABE process, product concentrations of alcohols are limited to approximately 20 g/L, as the presence of alcohols at concentrations higher than this can inhibit production, and it is toxic to the microorganisms in the fermentation broth [5]. These low product titers and also the higher boiling point of butanol than the boiling point of water make the costs of distillation tremendously high [7]. Consequently, the development of efficient downstream processing is essential if we are to reduce the costs of such processes. Adsorption in porous materials is an interesting alternative downstream processing method that is less energy demanding, even for low product titers [1, 8–10]. This makes the utilization of porous materials economically attractive and sustainable [2, 8–14], and thus adsorption in zeolites could be a promising method of recovering bioalcohols from the fermentation broth. In addition to downstream processing, zeolites can be used as catalysts; here, adsorption is the first step that initiates the reaction.

Therefore, the zeolite-catalyzed conversion of (bio-based) alcohols into biofuels, biochemicals, or gasoline is an interesting approach for extending the variety of products based on biomass-derived alcohols [3, 4, 8, 15, 16].

Zeolites are selective and stable microporous aluminosilicates with a periodic three-dimensional framework consisting of AlO_4 and SiO_4 tetrahedrons (T). The hydrophilic Al sites offer potential binding sites for the adsorption of organic molecules. Several experimental studies on the adsorptive recovery of fermentative products from aqueous solutions have been published [2, 12, 13]. The performance of zeolites in adsorptive product recovery depends on the diffusion and adsorption of molecules in the zeolite framework [17], whereas the porous framework structure delivers shape and size selectivity [17–19] by acting as a molecular sieve. Thus, larger molecules from the aqueous phase, such as proteins in the fermentation broth, are too big to enter the pores of the zeolite, meaning that these molecules cannot be adsorbed by the zeolite. In the context of alcohol recovery, MFI-type zeolite (MFI) is the most widely used type of zeolite, and so its framework has been thoroughly investigated. Other zeolite types are much more rarely discussed. However, zeolites such as BEA and MOR exhibit frameworks with slightly larger pore sizes, so they could represent alternative adsorbent materials that permit the adsorption of larger alcohols such as butanol. When investigating the adsorption potential of such materials, computational methods can be applied to gain new and useful molecular insights into the adsorption mechanisms [18, 20–24].

Alcohol adsorption was shown to preferentially occur at the Al sites in zeolite pores [3, 25–27]. This is due to (a) electrostatic interactions between the Al sites on the zeolite and the hydroxyl groups on the alcohol molecules, and (b) dispersion interactions between the zeolite lattice and the alcohol molecules [18, 28], which increase linearly by 2–4 kcal mol^{-1} per C atom on the alcohol [3, 4, 21]. Thus, long-range interactions based on dispersion forces are an important influence on the adsorption of alcohols in zeolites [25], which means that we must account for dispersion forces if we are to accurately describe the adsorption mechanism [18, 21, 25, 29]. Computationally, second-order Møller–Plesset perturbation theory (MP2) calculations yield adsorption energies of organic compounds in zeolites that are close to those observed experimentally, but this approach is computationally demanding, which restricts its application to large systems such as zeolites [22, 30]. Another approach is density functional theory (DFT), which is a good option for modeling extended and complex molecular systems considering the computational power and accuracy required [18, 22, 31, 32]. Thus, DFT is currently the method of choice for studying zeolites by means of quantum chemical calculations. However, it is commonly known that DFT using classical local-density or gradient-corrected density functionals is unable to account for dispersion forces deriving from long-range interactions. Therefore, several approaches have been developed over the last two decades to account for dispersion forces in DFT calculations [33–37]. One of the most popular and successful of these approaches is described by Grimme [33] (DFT-D2), and the data computed using this particular approach have shown good agreement with their corresponding experimental data in various studies [3, 4, 21].

Although the binding of alcohols in zeolites has been investigated intensively at the molecular level, the nature and stability of the resulting adsorption complexes are still topics of some debate. Two different binding complexes are described in the literature [3, 4, 17, 19–21, 23, 38–48]: (a) a neutral physisorption complex containing an H bond between the Al–OH and the OH of the alcohol, and (b) an ion-paired chemisorption complex that involves H transfer from the Al–OH to the OH of the alcohol (Fig. 1). In two of the most recent DFT studies, both types of complexes were found to be stable for various alcohols in MFI, and an equilibrium between them was suggested by the authors [3, 4]. However, these assumptions are restricted to MFI; molecular level information from systematic studies of other zeolites are—to the best of our knowledge—not available yet.

The DFT study described in the present paper was performed to obtain molecular level information on the adsorption of C1–C4 alcohols in BEA and MOR. Also, as most of the theoretical studies available in the literature have considered the MFI framework, the study reported here was an extension of prior works [3, 4, 17, 19–21, 23, 38–48] that was performed to investigate if the knowledge available for MFI is transferable and valid for other zeolite frameworks, such as BEA and MOR. For this study, cluster cutouts of the BEA and MOR framework were designed that contained the main structural elements of their pore channel frameworks. To investigate the quality of the cluster calculations, the results they gave were compared to those provided by periodic calculations. DFT-D was used in both approaches. In order to demonstrate that alcohols preferentially bind to Al sites in these two zeolites, the adsorption energies for models without Al sites were calculated and compared to those of Al-containing models. Population analysis and vibrational analysis were conducted to support the interpretation of the calculated geometries. MFI was included in this study to benchmark our computational procedure.

Experimental section

Chemicals

Zeolite BEA was provided by Süd-Chemie (now Clariant; Munich, Germany), and zeolite MOR was purchased from Tosoh Europe B.V. (Amsterdam, The Netherlands). Methanol

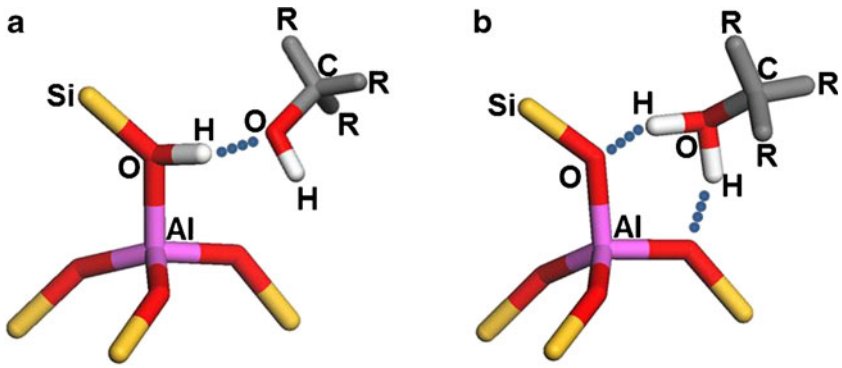

Fig. 1 Adsorption complexes of alcohols at zeolite Al sites: **a** physisorbed complex and **b** chemisorbed complex. R = side chain of the alcohol

(>99.9 %), 1-propanol (>99.5 %), and 2-propanol (> 99.8 %) were purchased from Carl Roth GmbH & Co. KG (Karlsruhe, Germany). Ethanol (> 99.9 %) was purchased from Merck KGaA (Darmstadt, Germany). 1-Butanol (>99.8 %) and 2-butanol (>99.7 %) were purchased from VWR International GmbH (Darmstadt, Germany). KH_2PO_4 (>99.0 %) and $MgSO_4 \times 7\ H_2O$ (>99.0 %) were purchased from Carl Roth GmbH & Co. KG. $FeSO_4 \times 7H_2O$ (>99.5 %), K_2HPO_4 (>99.0 %) and $(NH_4)_2SO_4$ (>99.5 %) were purchased from Merck KGaA. $MnSO_4 \times H_2O$ (>99 %) and NaCl (>99.5 %) were purchased from VWR International GmbH.

Preparation of the zeolites

BEA is a synthetic zeolite of the disordered zeolite beta family. Its three-dimensional framework contains 12-ring channel pores and two perpendicular straight channel pores with cross-sections of 7.6×6.4 Å [49]. The zeolite BEA used in this study had an atomic ratio of Si/Al = 12.5 and a BET surface of 550 m^2/g. The framework of zeolite MOR exhibits a one-dimensional 12-ring pore structure connected by eight-ring channels with diameters of 6.5×7.0 Å [50–52]. The zeolite MOR used in this study has an atomic ratio of Si/Al = 15 and a BET surface of 400 m^2/g. The zeolites were activated in nitrogen atmosphere for 24 h at 723.15 K.

Adsorption experiments

Because the fermentative production of alcohols using bacteria is limited to titers of approximately 20 g/l [5], the adsorption of alcohols from diluted aqueous solutions was investigated. Alcohol–water solutions were prepared with concentrations of 1 %, 2 %, 3 %, 5 %, and 7.5 % (vol/vol). Additionally, the adsorption by zeolite of alcohols from a dilute aqueous salt solution was measured to mimic real fermentation conditions to a first approximation. This solution contained salts (see Table S1 of the "Electronic supplementary material," ESM) from the *Clostridium* growth medium (CGM) [53] used in the ABE process [53–55]. In real fermentative production, carbon and nitrogen sources are required to maintain biochemical growth and production. Here, however, these educts were neglected, as we assumed that they were reduced to minimal levels by the end of the fermentation process.

For the adsorption experiments, 100 mg of zeolite and 1 ml of the alcohol–water solution were used, respectively. The adsorption experiments were performed on a lab rotator spinning at 25 rpm (Grant-bio PTR60, Grant Instruments, Shepreth, UK) at 298.15 K for 24 h to ensure that thermodynamic equilibrium was attained. The suspensions were then centrifuged at 12,000 rpm for 5 min (5415R microcentrifuge, Eppendorf AG, Hamburg, Germany) and the alcohol concentration in the supernatant was determined via uHPLC with a refractive index detector (1290 Infinity LC, Agilent Technologies, Santa Clara, CA, USA). An EC 125/3 Nucleodur C18 Pyramid column with 5 μm particles purchased from Macherey-Nagel GmbH & Co. KG (Dueren, Germany) was used. One microliter of the sample was injected, a 20 mM KH_2PO_4 buffer (pH 2 to pH 3) was used as eluent in the isocratic mode, and the flow was maintained at 1.5 ml/min.

Computational details

Alcohol models and DFT settings

Prior to the adsorption studies, the geometries of the C1–C4 alcohols (see Fig. S1 of the ESM for final geometries) were optimized by identifying their lowest-energy conformations on the potential energy surface. Geometry optimizations were carried out with the all-electron density functional program $DMol^3$ [56, 57] in Materials Studio 6.0 (Accelrys Inc., San Diego, CA, USA) [58] using the PBE exchange-correlation functional [59, 60] and the double numerical plus polarization (DNP) basis set [57]. Optimization was considered to have converged when the following convergence criteria were met: 1.0×10^{-5} Ha for the total energy, 0.002 Ha/Å for the maximum force on atoms, and 0.005 Å for the maximum atomic displacement. Long-range interactions between the zeolite framework and adsorbing molecules are known to be an

important influence on the adsorption behavior (see above). Thus, long-range dispersion interactions were included using the Grimme method [33] (DFT-D2), which was shown to be sufficient to study the adsorption of various small molecules in zeolites [3, 4, 21, 32]. These settings were used for all of the DFT results presented throughout this paper.

Zeolite models

Zeolites are aluminosilicates with a complex three-dimensional framework consisting of AlO_4 and SiO_4 tetrahedrons (T). The tetrahedrons of the crystalline network are linked to each other by shared oxygen atoms. The framework has a net negative charge due to each AlO_4 tetrahedron, and this charge is compensated by the presence of cations outside the framework [52].

Zeolite MFI

MFI was included in the study in order to benchmark the computational procedure with data from the literature. MFI consists of straight channel pores and zigzag channels. The 33 T cluster model of MFI was adapted from Hansen [61] in its unoptimized state, and geometry optimization was carried out using DMol^3 (see above). Figure S2 of the ESM shows the cluster in a unit cell of MFI, including one Al site. The net negative charge is compensated by the presence of an extra proton attached to an O atom neighboring the Al site.

Zeolite BEA

A 42 T cluster was designed as a small cutout of the BEA framework that still contained the intersection between the 12-ring channel pores in the three-dimensional framework. The Al site was inserted on the basis of the most stable geometry according to Fujita et al. [51]. The net negative charge was compensated by an extra proton attached to an O atom neighboring the Al site. For periodic calculations, the BEA structure (unit cell parameters a = 1.26 nm, b = 1.26 nm, c = 2.62 nm) was taken from the Materials Studio 6.0 structure database and the Al site was inserted at the same position as in the 42 T cluster (Fig. 2). This resulted in the chemical formula $H[AlSi_{63}O_{128}]$ per unit cell, the geometry of which was fully optimized. The 42 T cluster and periodic structures were used as models approximating the BEA used experimentally ($\sim H_5[Al_5Si_{59}O_{128}]$). By having only one Al site in one single pore, we were able to focus on a single defect without having to deal with several adsorbates or several interacting defect sites.

Zeolite MOR

A 33 T cluster was designed as a small cutout of the MOR framework which still contained a 12-ring channel pore that had dimensions deep enough to incorporate C1–C4 alcohols.

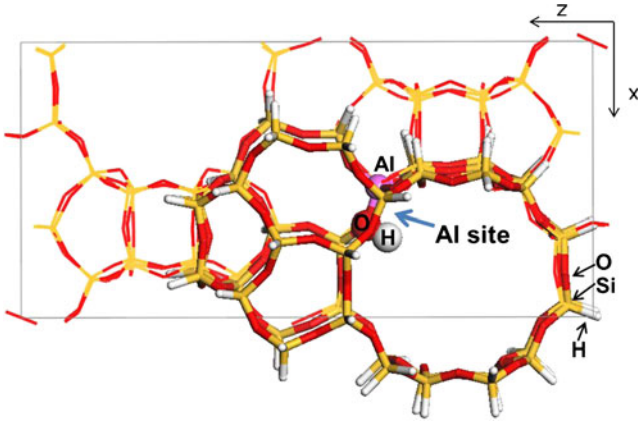

Fig. 2 View along the y-axis of the unit cell and the 42 T cluster model of BEA. Cluster atoms are drawn using *thick lines*, and the cluster is located in the periodic unit cell. The positions of the Al site atoms are presented as *spheres*

The Al site was inserted on the basis of the most stable geometry, as determined by geometry optimization with the Al site at all 12 T sites comprising the 12-ring channel. The net negative charge was compensated by the presence of an extra proton attached to an O atom neighboring the Al site. For periodic calculations, the MOR structure (unit cell parameters a = 1.81 nm, b = 2.05 nm, c = 0.75 nm) was taken from the Materials Studio 6.0 structure database and the Al site was inserted at the same position as in the 33 T cluster (Fig. 3). This resulted in the chemical formula $H[AlSi_{47}O_{96}]$ per unit cell, the geometry of which was fully optimized. The 33 T cluster and periodic structures were used as models approximating the experimentally used MOR ($\sim H_3[Al_3Si_{45}O_{96}]$).

Al-free cluster and periodic models of BEA (see Fig. S3 of the ESM) and MOR (see Fig. S4 of the ESM) were created by

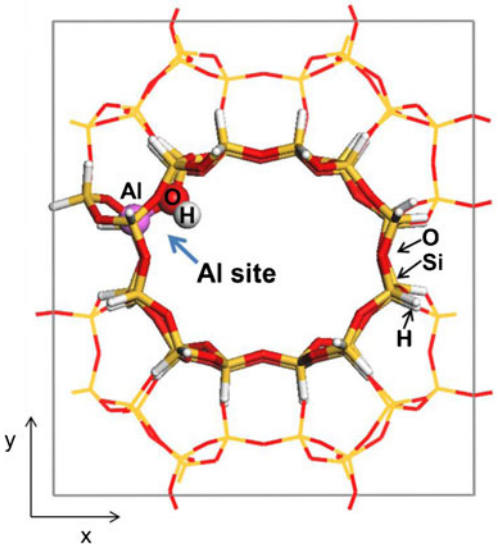

Fig. 3 View along the z-axis of the unit cell and the 33 T cluster model of MOR. Cluster atoms are drawn using *thick lines*, and the cluster is located in the periodic unit cell. The positions of the Al site atoms are presented as *spheres*

replacing Al with Si and removing the charge-compensating hydrogen.

Geometry optimization of complexes

For adsorption studies of alcohols in zeolites, the geometries of complexes consisting of one alcohol molecule per zeolite model were optimized. Total adsorption energies (ΔE_{ads}) in the gas phase were calculated via

$$\Delta E_{ads} = E_{complex} - E_z - E_{alc}, \quad (1)$$

where $E_{complex}$ is the optimized total energy of alcohol in the zeolite model, E_z is the total energy of the zeolite model, and E_{alc} is the total energy of the alcohol. Thermodynamic data were computed for cluster calculations of zeolite–alcohol complexes by performing vibrational analysis in DMol[3] and adding the specific term for the enthalpy (ΔH_{ads}) at $T = 298$ K to the computed electronic energy (ΔE_{ads}).

Cluster calculations In order to restore the electrical field and to provide the pristine zeolite framework with structural rigidity, constraints were set on particular atoms of the cluster models during all geometry optimizations. For MFI, the terminating H atoms and the $OSiH_3$ group terminating the Al site were constrained. For BEA and MOR, constraints were set for the terminating H atoms. The remaining atoms of the cluster models and the alcohol atoms were allowed to relax.

Periodic calculations For all zeolites, the lattice atoms and alcohol atoms were allowed to relax but the parameters of the unit cell were kept constant.

Results

Computational results

Geometries and adsorption energies in Al-containing zeolites

In order to check that the chosen DFT approach delivers reliable results, the physisorption of C1–C3 alcohols in an MFI 33 T cluster was investigated and compared to experimental and theoretical data from the literature. C1–C3 alcohols were considered because appropriate experimental results on adsorption were only available for these alcohols [27]. The calculated adsorption energies and the literature data [3, 21, 27] show only small deviations from each other (Table 1). Hence, it can be assumed that the chosen DFT approach is applicable for studying the adsorption of alcohols in BEA and MOR too.

Table 1 Adsorption energies (in kcal mol^{-1}) of C1–C3 alcohols in an Al-containing zeolite MFI cluster

Alcohol	$\Delta H_{exp.}$[a]	$\Delta H_{comp.}$[b]	$\Delta E_{Lit.}$[c]	$\Delta E_{ads\_cluster}$[d]
Methanol	−27.5±1	−25.8	−27.0	−27.2
Ethanol	−31.0±1	−29.6	−29.9	−31.3
1-Propanol	−34.6±1	−33.4	−32.2	−36.2

[a] Experimental values from [27]. [b] Cluster results from [21]. [c] Periodic results from [3]. [d] Cluster results from this study. [b–d] Values for physisorbed states

For the adsorption of C1–C4 alcohols in BEA and MOR, complexes of physisorbed and chemisorbed alcohols in the pores of the zeolite were obtained. Various initial positions of the alcohols in the alcohol–zeolite complexes were chosen by chemical intuition and their geometries were optimized. Results presented in the following refer to the most stable states only. Cluster calculations produced adsorption energies (ΔE_{ads}) that were very close to the results obtained from periodic calculations (Table 2). In comparison to the physisorbed complexes, the chemisorbed analogs were found to be more stable by 2–7 kcal mol^{-1} and 2–4 kcal mol^{-1} in the cluster and periodic calculations, respectively. The adsorption energies increased by 2–5 kcal mol^{-1} per additional carbon atom in the alcohol molecule in both the physisorbed and chemisorbed complexes. The geometries obtained from cluster and periodic calculations were very similar to each other (see Figs. S5–S8 of the ESM), suggesting that the cluster cutouts of BEA and MOR provide accurate descriptions of the overall bonding environment. Figures 4 and 5 schematically demonstrate the two different adsorption complexes of the physisorbed and chemisorbed alcohols in BEA, and MOR, respectively.

The conclusion derived from the calculated geometries that two different adsorption complexes of alcohols in BEA and MOR are formed is further supported by population analysis results. For example, the Hirshfeld [62] or Mulliken [63] charge partitioning method can be used to represent charge distributions of molecular entities. Mayer bond order calculations can also yield information on molecular bonding [64]. Figures 6 and 7 show the zeolite atoms included in the evaluation of Hirshfeld charges and Mayer bond orders for BEA and MOR (respectively) cluster calculations. According to the data obtained, the adsorption of alcohols affects the proximity of the zeolite Al site (Al, H1, and O1–O4, Figs. 6 and 7). Atoms H1 and O1 in BEA and MOR are the most heavily involved in binding the alcohols, as illustrated by the significant changes in the Mayer bond orders for both binding mechanisms. The O1–H1 bond order drops sharply when the proton is transferred from the Al site to the OH group on the alcohol during chemisorption (Figs. 6a and 7a). During physisorption, the decrease in the bond order of the O1–H1

Table 2 Computed total adsorption energies (ΔE_{ads}, in kcal mol^{-1}) of C1–C4 alcohols physisorbed and chemisorbed in Al-containing BEA and MOR

Alcohol	BEA				MOR			
	Physisorbed		Chemisorbed		Physisorbed		Chemisorbed	
	Cluster	Periodic	Cluster	Periodic	Cluster	Periodic	Cluster	Periodic
Methanol	−25.5	−26.2	−29.9	−27.7	−26.1	−26.1	−28.7	−28.1
Ethanol	−28.9	−30.9	−34.2	−33.2	−29.4	−30.3	−32.7	−33.3
1-Propanol	−31.6	−34.0	−36.6	−36.4	−34.0	−33.9	−35.8	−37.5
2-Propanol	−30.7	−33.5	−37.3	−37.3	−33.2	−34.5	−36.7	−37.6
1-Butanol	−33.8	−37.0	−39.6	−40.7	−35.6	−37.4	−37.8	−39.2
2-Butanol	−32.9	−37.3	−39.5	−39.6	−35.1	−37.2	−39.4	−41.2

bond is less significant (Figs. 6b and 7b). If we consider the Hirshfeld charges, the charge on O1 becomes more negative and that on H1 becomes less positive as a result of adsorption. This effect was stronger in the case of chemisorption with proton transfer from the zeolite Al site to the OH group of the alcohol (Figs. 6 and 7). The Hirshfeld charge on H1 due to adsorption in both the chemisorbed and the physisorbed states.

Vibrational analysis

Vibrational analysis was conducted to explore the relationship between the frequencies of the calculated geometries for BEA and MOR obtained in this study and the frequencies of zeolite–alcohol complexes reported in the literature. The data for the chemisorbed and physisorbed alcohol–zeolite cluster complexes were subsequently evaluated by visualizing the particular vibrational modes using the Vibrational Analysis Tool in Materials Studio 6.0. In the cluster calculations, constraints were placed on the terminating H atoms during optimizations. It should be mentioned that these constraints led to the occurrence of small imaginary frequencies, although these imaginary frequencies did not influence the vibrations of the adsorption site in the zeolite and the alcohols.

The most meaningful modes and corresponding frequencies are shown in Tables 3, 4, 5, and 6. The adsorption of alcohols on different zeolites and the resulting shifts in the vibrational frequencies have been discussed intensively In the literature [3, 4, 38, 42, 43, 45, 65–72]. Qualitatively comparable frequencies and frequency shifts were observed for the binding of alcohols in the pores of zeolite BEA (Tables 3 and 5) and zeolite MOR (Tables 4 and 6). No significant shifts in the stretching and bending modes of the CH and CH_3 of the alcohol were observed in the chemisorbed and physisorbed complexes. However, significant shifts in the frequencies of the OH groups of the zeolite–alcohol complexes were observed. In the case of physisorption, a proton is transferred from the zeolite to the OH group of the alcohol. In this situation, strong shifts in the stretching frequencies of the alcohol OH and the zeolite OH to lower wavenumbers were observed, whereas the bending modes of the zeolite were shifted to higher wavenumbers. In chemisorption, a proton is transferred from the zeolite to the OH group of the alcohol, resulting in OH_2^+. Due to this proton transfer, the symmetric and asymmetric stretching modes of the OH_2^+ group on the alcohol were observed at lower wavenumbers than for the native alcohol and zeolite. In addition, a bending mode of the OH_2^+ group on the alcohol was observed. The frequencies

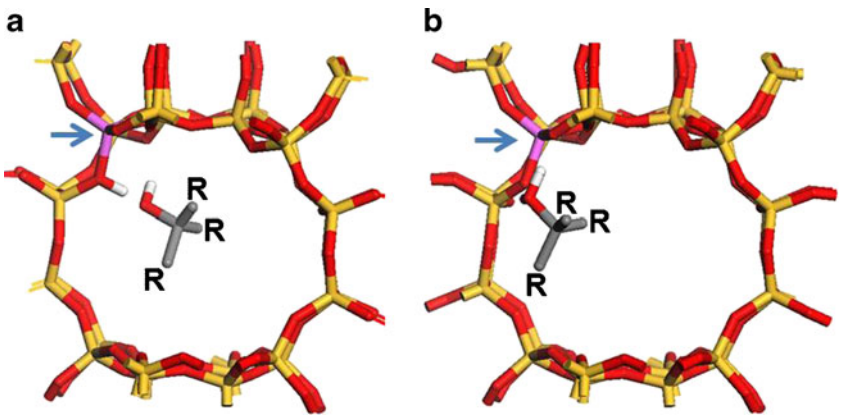

Fig. 4 Adsorption of alcohols in zeolite BEA. The geometries of **a** physisorbed and **b** chemisorbed complexes in the pores of BEA are shown schematically. R=side chain of the alcohol

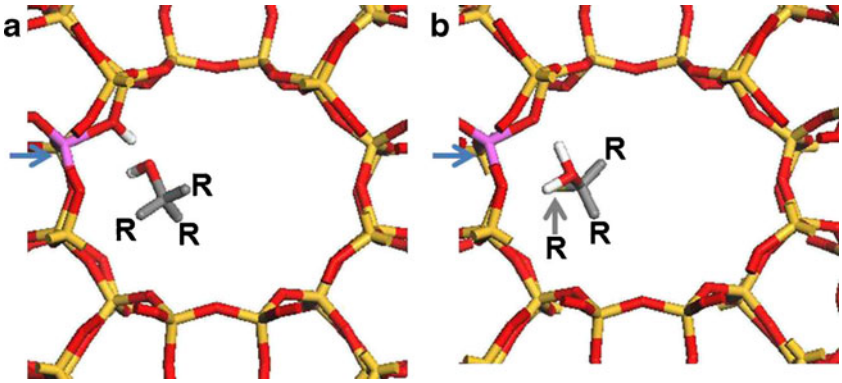

Fig. 5 Adsorption of alcohols in zeolite MOR. The geometries of **a** physisorbed and **b** chemisorbed complexes in the pore of MOR are shown schematically. R = side chain of the alcohol. *Arrows* point at the Al site of the zeolite model

and corresponding shifts obtained here were in the same range as the frequencies and shifts reported for alcohol adsorption in zeolites in the literature; e.g., see [3, 4, 43] for details.

In addition to frequencies, thermodynamic properties such as the enthalpy (ΔH_{ads}) can be obtained from vibrational analysis by incorporating zero-point vibrational energy correction (ZPE) as well as translational, vibrational, and rotational contributions. Enthalpies were calculated for the cluster–alcohol complexes of BEA and MOR (see Figs. S5–S8 of the ESM) at a temperature of 298.15 K; these are depicted in Figs. S9 and S10 of the ESM. A linear relationship between the adsorption energy (ΔE_{ads}) and enthalpy (ΔH_{ads}) was observed (see Figs. S9 and S10 of the ESM).

Geometries and adsorption energies in Al-free zeolites

The adsorption of alcohols in zeolites has already been reported to occur primarily at zeolite Al sites [3, 25–27]. Proof of this comes from the fact that the adsorption energies of various alcohols differ depending on whether the adsorption occurs in Al-free or Al-containing MFI—the energies associated with Al-containing MFI are higher [3]. In order to check that this observation is correct for BEA and MOR, the adsorption energies of alcohols binding in Al-free zeolite models were calculated and compared to those for Al-containing ones. The corresponding adsorption energies for the cluster models are shown in Table 7. For both zeolites, the adsorption energies

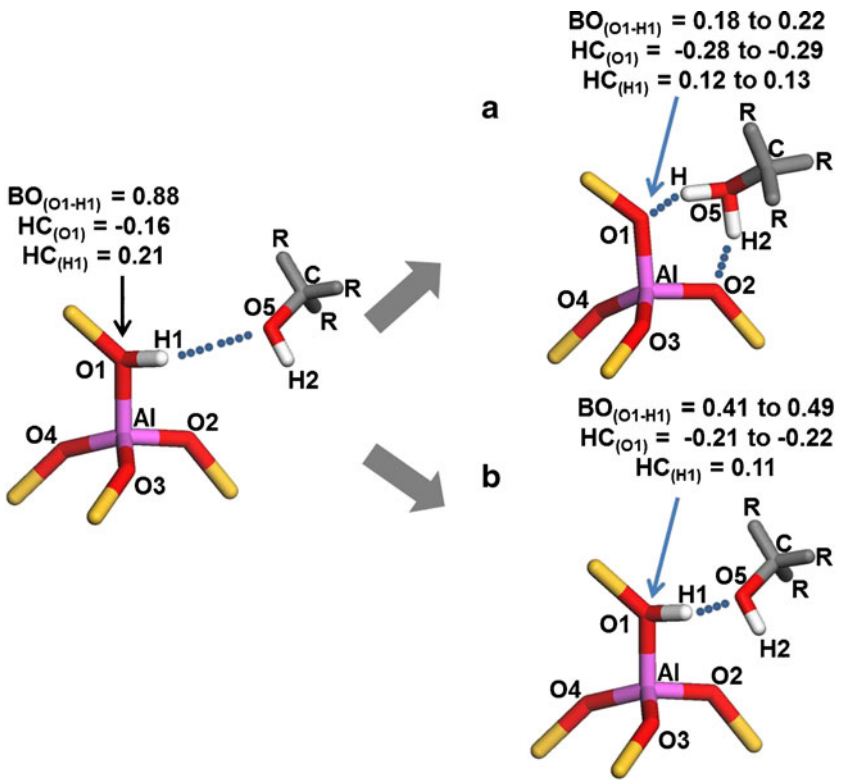

Fig. 6 Schematic binding complexes of alcohols in BEA following **a** chemisorption and **b** physisorption. Atoms in the neighborhood of the BEA Al site that were taken into account in the population analysis are labeled. $BO_{(O1–H1)}$ Mayer bond orders for O1 and H1, *HC* Hirshfeld charges for O1 and H1. R = side chain of the alcohol. *Arrows* point at the Al site of the zeolite model

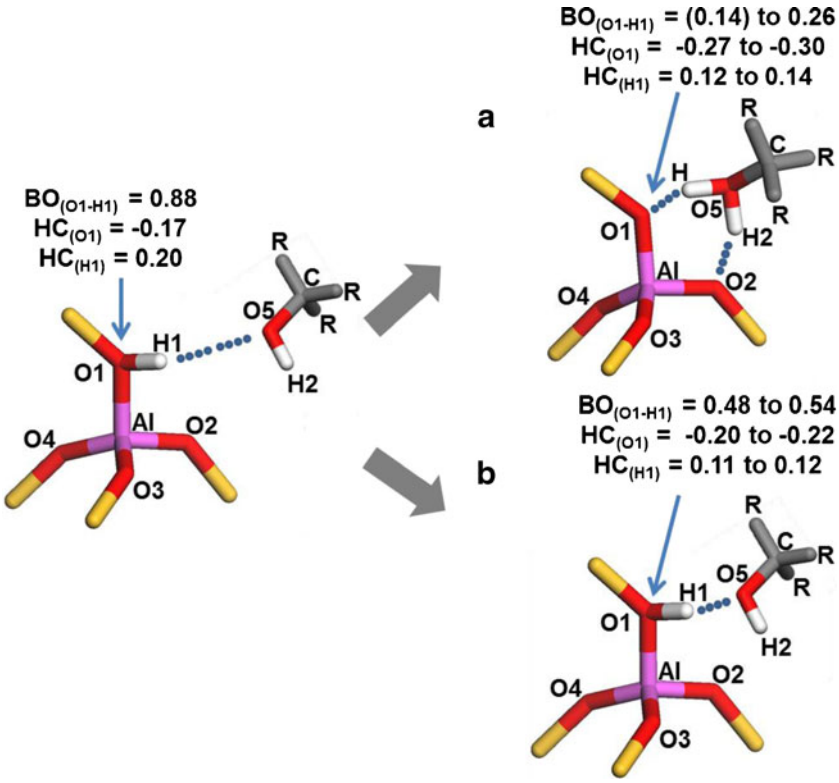

Fig. 7 Schematic binding complexes of alcohols in MOR following **a** chemisorption and **b** physisorption. Atoms in the neighborhood of the MOR Al site that were taken into account in the population analysis are labeled. $BO_{(O1–H1)}$ Mayer bond orders for O1 and H1, *HC* Hirshfeld charges for O1 and H1. R = side chain of the alcohol

increased as the number of C atoms in the alcohol increased. Thus, the weakest interactions were noted for methanol, and the strongest interactions for the butanol isomers. Additionally, the adsorption energies were significantly (12–16 kcal mol^{-1}) lower for both Al-free zeolite models (Table 7). These results are consistent with data on MFI available from the literature [3].

Experimental adsorption isotherms

The linear slope of an adsorption curve close to its origin is an important characteristic that tells us about the affinity between the alcohol and the zeolite at low concentrations. The steeper the slope, the higher the affinity and the corresponding loading of the zeolite. Thus, by comparing the initial slopes of

Table 3 Calculated frequencies of C1–C4 alcohols adsorbed on BEA, leading to physisorbed complexes

Species	CH stretching	CH bending	CH_3 bending	Alcohol OH stretching	Zeolite OH stretching[a]	Zeolite OH bending* (in-plane)
BEA					3661	1147
MeOH	3083–2948	1484–1461	1445	3726		
MeOH	3092–2971	1480–1448	1391	3395	1781	1391
EtOH	3099–2932	1486–1402	1357	3731		
EtOH	3057–2958	1472–1425	1371	3334	1645	1425
1-Propanol	3104–2937	1499–1421	1390	3744		
1-Propanol	3056–2961	1487–1447	1352	3359	1646	1427
2-Propanol	3087–2925	1474–1435	1381	3723		
2-Propanol	3065–2962	1482–1385	1360	3607	1837	1452
1-Butanol	3068–2936	1474–1385	1370	3715		
1-Butanol	3055–2929	1494–1436	1390	3596	1707	1494
2-Butanol	3097–2929	1473–1401	1366	3719		
2-Butanol	3072–2955	1489–1438	1391	3485	1639	1444

[a] Bending and stretching modes of the zeolite OH were observed to be coupled

Table 4 Calculated frequencies of C1–C4 alcohols adsorbed on MOR, leading to physisorbed complexes

Species	CH stretching	CH bending	CH_3 bending	Alcohol OH stretching	Zeolite OH stretching[a]	Zeolite OH bending* (in-plane)
MOR					3642	1116
MeOH	3083–2948	1484–1461	1445	3726		
MeOH	3087–2978	1472–1439	1403	3663	2085	1403
EtOH	3099–2932	1486–1402	1357	3731		
EtOH	3063–2963	1473–1454	1399	3656	1990	1410
1-Propanol	3104–2937	1499–1421	1390	3744		
1-Propanol	3085–2956	1494–1460	1407	3618	1648	1446
2-Propanol	3087–2925	1474–1435	1381	3723		
2-Propanol	3063–2957	1476–1443	1389	3648	1740	1420
1-Butanol	3068–2936	1474–1385	1370	3715		
1-Butanol	3053–2945	1487–1395	1375	3624	1917	1519
2-Butanol	3097–2929	1473–1401	1366	3719		
2-Butanol	3065–2940	1473–1430	1381	3691	2039	1487

[a] Bending and stretching modes of the zeolite OH were observed to be coupled

different adsorption curves, we can get an idea of the affinities between the alcohols and zeolites. Figure 8a shows the adsorption behavior of C1–C4 alcohols in zeolite BEA. Taking the initial slope into account, the affinities of the different alcohols for BEA appear to increase in the following order: methanol < ethanol < (1-propanol ~ 2-propanol) < (1-butanol ~ 2-butanol). The maximum loadings were approximately $q = 0.0016$ mol/g for C2–C4 alcohols and $q = 0.0014$ mol/g for methanol. These results were found to be comparable to the actual adsorption behavior of alcohols from aqueous salt solution (Fig. 8b).

For MOR (Fig. 9a), the affinities of the different alcohols for MOR conform to the following trend: ethanol < (1-propanol ~ 2-propanol) < (1-butanol ~ 2-butanol) < methanol. The maximum loadings were approximately $q = 0.001$ mol/g for methanol, $q = 0.0005$ mol/g for ethanol, and less than $q = 0.0003$ mol/g for C3 and C4 alcohols. The adsorption behavior of alcohols from aqueous salt solution (Fig. 9b) was comparable to that seen for the alcohols from aqueous solution.

Discussion

Theoretical modeling approaches using static quantum chemical calculations such as DFT are widely used to gain a deeper understanding of and support experimental work focusing on adsorption processes on the surfaces of materials such as zeolites [18, 21, 73]. Furthermore, molecular level information can be used to support the design of efficient adsorption processes by predicting trends in adsorption behavior. By conducting DFT calculations, useful quantities such as adsorption energies and geometries can be computed straightforwardly and efficiently. This is important because trends in the adsorption affinity that can be used to elucidate a relative scale of stability for the adsorption complexes can be obtained when the adsorption energies are known [74]. The present study investigated the adsorption of C1–C4 alcohols in the zeolites BEA and MOR using judiciously designed computational models at the DFT level of theory to gain new molecular insights that can aid the rational design of adsorbent materials

Table 5 Calculated frequencies of C1–C4 alcohols adsorbed on BEA, leading to chemisorbed complexes

Alcohol	CH stretching	CH bending	CH_3 bending	Alcohol OH stretching		Alcohol OH bending
				Symmetric	Asymmetric	
MeOH	3136–2991	1467–1453	1429	2787	1975	1652
EtOH	3097–2984	1474–1447	1407	2971	1915	1619
1-Propanol	3074–3038	1471–1410	1376	3002	1886	1601
2-Propanol	3068–2966	1479–1444	1393	2771	2284	1683
1-Butanol	3061–2933	1472–1448	1402	2981	1921	1607
2-Butanol	3063–2970	1485–1429	1382	2800	2290	1687

Table 6 Calculated frequencies of C1–C4 alcohols adsorbed on MOR, leading to chemisorbed complexes

Alcohol	CH stretching	CH bending	CH_3 bending	Alcohol OH stretching		Alcohol OH bending
				Symmetric	Asymmetric	
MeOH	3102–2986	1478–1453	1432	2678	2065	1684
EtOH	3082–2983	1476–1464	1408	2706	2236	1702
1-Propanol	3062–2946	1480–1395	1364	2663	2313	1702
2-Propanol	3073–3975	1478–1444	1398	2689	2459	1694
1-Butanol	3062–2939	1485–1386	1373	2750	2245	1687
2-Butanol	3071–2949	1482–1445	1388	2752	2385	1686

[16] and adsorption processes. DFT with PBE + D (see above) was used, which was shown to perform well in describing the adsorption characteristics of zeolites [3, 4, 21, 31, 32]. However, in order to demonstrate the adequacy of these DFT settings, MFI cluster calculations were included and compared to available literature data. Adsorption energies for C1–C3 alcohols, namely methanol, ethanol, and 1-propanol, in the straight channel pore of MFI were calculated and found to be comparable with experimental [27] and DFT [3, 21] data from the literature (Table 1). These results suggest that the calculated gas-phase adsorption energies for BEA and MOR should be reliable, too.

The balance between accuracy and the computational resources required is an important consideration in molecular modeling. This means that it is necessary to choose an appropriate compromise between accuracy and computational costs—both of which depend on the size of the model chosen. Alcohols are small organic molecules of a given particular size, but different models can be applied for zeolites. Cluster models represent cutouts of the zeolite framework, which have been shown to work well for different organic molecules; e.g., see [21, 75–78]. Periodic calculations have the advantage of accounting for the full framework and the complete long-range interaction potential [41]. As the differences in corresponding adsorption energies (Table 2) and geometries (see Figs. S5–S8 of the ESM) between cluster and periodic calculations are very small, and the physicochemical picture remains unchanged, the cutouts of the cluster models represent a sufficiently large approximation of the periodic framework that minimizes the computational effort required.

Table 7 Computed total adsorption energies[a] (ΔE_{ads}, in kcal mol^{-1}) of C1–C4 alcohols in Al-free periodic BEA_{Al_free} and MOR_{Al_free}, and the differences in adsorption energy[b] from the corresponding energies obtained for Al-containing BEA_{Al} and MOR_{Al}

Alcohol	BEA_{Al_free}[a]	$BEA_{Al\text{-}Al\_free}$[b]	MOR_{Al_free}[a]	$MOR_{Al\text{-}Al\_free}$[b]
Methanol	−12.0	−14.2	−13.8	−12.3
Ethanol	−14.9	−16.0	−16.5	−13.8
1-Propanol	−21.2	−12.8	−21.0	−12.9
2-Propanol	−20.6	−12.9	−20.4	−14.1
1-Butanol	−23.8	−13.2	−23.5	−13.9
2-Butanol	−23.5	−13.8	−22.4	−14.8

[b] Calculated by subtracting ΔE_{ads} for the Al-free complex from ΔE_{ads} for the Al-containing complex

The calculated adsorption energies of alcohols in BEA and MOR increased with the number of C atoms in the alcohol, due to stronger long-range interactions with the zeolite framework. The following trend in adsorption energies in BEA and MOR was obtained via DFT: methanol < ethanol < (1-propanol < 2-propanol) < (1-butanol < 2-butanol). This is in good accord with the results of studies from the literature [21, 25], which reported that dispersion forces from interactions between the adsorbate and the zeolite lattice cause the adsorption strength to increase by 3–4 kcal mol^{-1} per additional C atom in the organic molecule adsorbed.

It is still a matter of debate [3, 4, 19, 38, 47, 48, 79] as to whether, and under which conditions, alcohols adsorb preferentially in a chemisorbed or physisorbed state in zeolites (Fig. 1). We were able to calculate both the chemisorbed and physisorbed states in BEA and MOR. This leads to the assumption that an equilibrium between both adsorption modes for the gas-phase adsorption of C1–C4 alcohols may exist for BEA and MOR, as also suggested for MFI; e.g., see [3, 4]. Evaluating the data derived from population analysis of the BEA and MOR cluster models gave further details regarding the molecular level binding mechanisms. The Al sites H1 and O1 in BEA and MOR were found to be mainly involved in binding the alcohols, as illustrated by the significant changes in Mayer bond orders seen for both binding mechanisms. The different binding situations were also supported by the occurrence of different shifts in the vibrational frequencies depending on the binding. The observed frequency shifts were consistent with literature data from both experimental and molecular modeling studies of alcohol adsorption at zeolite Al sites [3, 4, 38, 42, 43, 45, 65–71].

In addition to frequency shifts, meaningful thermodynamic properties such as the enthalpy (ΔH_{ads}) can be obtained from vibrational analysis by incorporating the zero-point

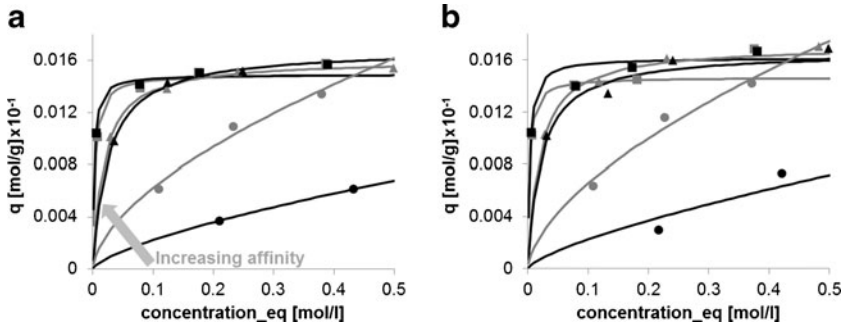

Fig. 8 Data from experiments studying the adsorption in zeolite BEA of alcohols **a** from aqueous solutions and **b** from aqueous salt solutions. The experimental results are shown as *symbols* and the fitted isotherms are depicted as *curves*. *Black circles* methanol, *gray circles* ethanol, *black triangles* 1-propanol, *gray triangles* 2-propanol, *black squares* 1-butanol, *gray squares* 2-butanol

vibrational energy correction as well as translational, vibrational, and rotational contributions. This is sometimes of particular interest, as DFT calculations can only provide internal energies at the athermal limit, $T = 0$ K. However, a linear relationship between adsorption energy ΔE_{ads} and adsorption enthalpy ΔH_{ads} calculated at 298 K was found for BEA (see Fig. S9 of the ESM) and MOR (see Fig. S10 of the ESM), which indicates that the usage of pure adsorption energy as a straightforward parameter for the prediction of adsorption strength is reasonable.

To investigate the influence of the interactions of alcohols with the Al site, adsorption energies of alcohols in pure siliceous BEA and MOR were calculated. The elimination of the Al sites from the zeolite models resulted in significantly lower adsorption energies. This suggests that the highest affinities between alcohols and BEA and MOR arise from interactions of the alcohols with Al sites in zeolites, as previously also described for MFI by Nguyen et al. [3].

The DFT data presented here provide the following new information: (a) the geometries of the adsorption complexes of alcohols in BEA and MOR for both physisorbed and chemisorbed states, (b) the corresponding adsorption energies, (c) comparable results from cluster and periodic calculations, (d) vibrational frequencies of the complexes, which show shifts comparable to those reported in the literature, and (e) a linear relationship between ΔE_{ads} and ΔH_{ads}. The extensive knowledge gained for MFI (i.e., in the most recent and well-conducted DFT studies by Nguyen et al. [3, 4] and van der Mynsbrugge et al. [21]), in combination with our data, suggests that gas-phase adsorption of alcohols in BEA and MOR takes place via the same underlying mechanisms described for MFI.

Apart from the theoretical considerations, we wanted to know if the knowledge obtained from DFT calculations can be used straightforwardly as a highly simplified model to predict the adsorption of alcohol from aqueous solution. Thus, the adsorption of alcohols from aqueous solution and from salt-containing aqueous solution was measured experimentally. The salt-containing solutions were used to imitate a real fermentation broth to a highly simplified first approximation. In general, for salt-containing aqueous solutions of alcohols, no effect of the salt on the adsorption of alcohols was observed, and their loadings on the zeolites were not influenced. Considering the slopes of the measured adsorption curves, the affinities of alcohols for BEA follow the same pattern as predicted with DFT: methanol < ethanol < (1-propanol ~ 2-propanol) < (1-butanol ~ 2-butanol). However, one negative observation must be commented on briefly here. For MOR, the calculated (methanol < ethanol < (1-propanol ~ 2-propanol) < (1-butanol ~ 2-butanol)) and experimental

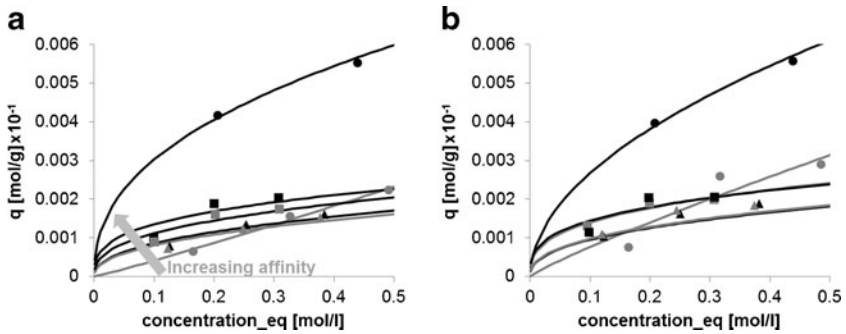

Fig. 9 Data from experiments studying the adsorption in zeolite MOR of alcohols **a** from aqueous solutions and **b** from aqueous salt solutions. Experimental results shown as *symbols* and the fitted isotherms are depicted as *curves*. *Black circles* methanol, *gray circles* ethanol, *black triangles* 1-propanol, *gray triangles* 2-propanol, *black squares* 1-butanol, *gray squares* 2-butanol

(ethanol < (1-propanol ~ 2-propanol) < (1-butanol ~ 2-butanol) < methanol) affinities differ. Moreover, the experimental maximum loadings in the two zeolite pores (BEA and MOR) differed from each other. In BEA, maximum loadings up to 0.0016 mol/g alcohol was found, which is consistent with literature data for adsorption of alcohols in microporous media [8, 10–14, 80]. In MOR, however, adsorption was restricted to about 0.001 mol/g methanol, and the loading strongly decreased with increasing side-chain length of the alcohol.

The different results for the adsorption of alcohols in BEA and MOR from aqueous solution underline that, in addition to the pure affinities between the alcohols and the zeolite lattice, other characteristics can also influence the adsorption behavior. Such characteristics could include steric hindrance [17–19, 48, 81] of the zeolite framework itself and diffusion effects [17]. BEA has pore channels that are approx. 7 Å in diameter and span a three-dimensional porous framework. MOR also exhibits pore channel diameters of approx. 7 Å; however, these pores exist in only one direction of the channel system. Thus, in MOR, steric hindrance may be more significant than in BEA. Furthermore, diffusion in MOR could be limited, as the largest pores in the framework are only accessible in one dimension. Another aspect could be different affinities of water clusters [23, 44, 82] for BEA and MOR, resulting in competition between water and alcohol molecules [17] at the zeolite Al sites. This could affect the desorption of water molecules from the zeolite Al sites that is required to clear the way for alcohol adsorption from aqueous solution. Thus, it may be worth investigating the co-adsorption of water and alcohols in zeolites in more detail, i.e., by taking molecular dynamics into account.

Conclusions

DFT calculations can enhance our understanding of molecular binding mechanisms by predicting adsorption energies and the orientations of molecules in the pores of zeolites during alcohol adsorption. The calculated adsorption energies and vibrational frequencies were found to be in the same ranges for particular alcohols in zeolite BEA and MOR. Small differences were observed in the corresponding adsorption energies and geometries obtained from cluster and periodic calculations of BEA and MOR, respectively. Thus, the cutouts of the two designed cluster models were large enough models of the periodic frameworks, meaning that they could be used for further adsorption studies in BEA and MOR. The adsorption energies and vibrational shifts obtained were comparable to those described in the literature for zeolite MFI, the most investigated and applied zeolite in this field of science and industry. This suggests that BEA and MOR are potential alternatives to MFI in terms of industrial applications. The adsorption of alcohols from an aqueous solution such as a fermentation broth is an especially interesting topic. The binding of alcohols from aqueous solution appears, however, to be somewhat more complex, and attempts to straightforwardly predict the binding behavior from simple gas-phase calculations were only partly successful. The pores in the framework and competitive water adsorption may exert significant influences on the adsorption of alcohols in microporous materials from aqueous solution.

Acknowledgments The research leading to these results has received funding from the Ministry of Innovation, Science and Research of North Rhine-Westphalia through the CLIB-Graduate *Cluster Industrial Biotechnology* initiative, contract no: 314–108 001 08.

References

1. Remy T, Cousin Saint Remi J, Singh R et al (2011) Adsorption and separation of C1−C8 alcohols on SAPO-34. J Phys Chem C 115(16): 8117–8125. doi:10.1021/jp111615e
2. Cousin Saint Remi J, Baron G, Denayer J (2012) Adsorptive separations for the recovery and purification of biobutanol. Adsorption 18(5–6):367–373. doi:10.1007/s10450-012-9415-1
3. Nguyen CM, Reyniers M, Marin GB (2010) Theoretical study of the adsorption of C1–C4 primary alcohols in H-ZSM-5. Phys Chem Chem Phys 12(32):9481. doi:10.1039/c000503g
4. Nguyen CM, Reyniers M, Marin GB (2011) Theoretical study of the adsorption of the butanol isomers in H-ZSM-5. J Phys Chem C 115(17):8658–8669. doi:10.1021/jp111698b
5. Oudshoorn A, van der Wielen LAM, Straathof AJJ (2009) Assessment of options for selective 1-butanol recovery from aqueous solution. Ind Eng Chem Res 48(15):7325–7336. doi:10.1021/ie900537w
6. Nielsen DR, Prather KJ (2009) In situ product recovery of *n*-butanol using polymeric resins. Biotechnol Bioeng 102(3):811–821. doi:10.1002/bit.22109
7. Qureshi N, Hughes S, Maddox IS et al (2005) Energy-efficient recovery of butanol from model solutions and fermentation broth by adsorption. Bioprocess Biosyst Eng 27(4):215–222. doi:10.1007/s00449-005-0402-8
8. Xiong R, Sandler SI, Vlachos DG (2011) Alcohol adsorption onto silicalite from aqueous solution. J Phys Chem C 115(38):18659–18669. doi:10.1021/jp205312k
9. Bai P, Tsapatsis M, Siepmann JI (2012) Multicomponent adsorption of alcohols onto silicalite-1 from aqueous solution: isotherms, structural analysis, and assessment of ideal adsorbed solution theory. Langmuir 28(44):15566–15576
10. Oudshoorn A, van der Wielen LAM, Straathof AJJ (2012) Desorption of butanol from zeolite material. Biochem Eng J 67:167–172
11. Oudshoorn A, van der Wielen LA, Straathof AJ (2009) Adsorption equilibria of bio-based butanol solutions using zeolite. Biochem Eng J 48(1):99–103. doi:10.1016/j.bej.2009.08.014
12. Delgado JA, Uguina MA, Sotelo JL et al (2012) Separation of ethanol–water liquid mixtures by adsorption on silicalite. Chem Eng J 180:137–144. doi:10.1016/j.cej.2011.11.026
13. Bowen TC, Vane LM (2006) Ethanol, acetic acid, and water adsorption from binary and ternary liquid mixtures on high-silica zeolites. Langmuir 22(8):3721–3727. doi:10.1021/la052538u
14. Saravanan V, Waijers D, Ziari M et al (2010) Recovery of 1-butanol from aqueous solutions using zeolite ZSM-5 with a high Si/Al ratio; suitability of a column process for industrial applications. Biochem Eng J 49(1):33–39. doi:10.1016/j.bej.2009.11.008

15. Bjørgen M, Svelle S, Joensen F et al (2007) Conversion of methanol to hydrocarbons over zeolite H-ZSM-5: on the origin of the olefinic species. J Catal 249(2):195–207. doi:10.1016/j.jcat.2007.04.006
16. Xiong R, Sandler SI, Vlachos DG (2012) Molecular screening of alcohol and polyol adsorption onto MFI-type zeolites. Langmuir 28(9):4491–4499. doi:10.1021/la204710j
17. Zhang K, Lively RP, Noel JD et al (2012) Adsorption of water and ethanol in MFI-type zeolites. Langmuir 28(23):8664–8673. doi:10.1021/la301122h
18. Brogaard RY, Moses PG, Nørskov JK (2012) Modeling van der Waals interactions in zeolites with periodic DFT: physisorption of *n*-alkanes in ZSM-22. Catal Lett 142(9):1057–1060. doi:10.1007/s10562-012-0870-9
19. Haase F, Sauer J (2000) Ab initio molecular dynamics simulation of methanol interacting with acidic zeolites of different framework structure. Microporous Mesoporous Mater 35–36:379–385
20. Wu JY, Liu QL, Xiong Y et al (2009) Molecular simulation of water/alcohol mixtures' adsorption and diffusion in zeolite 4A membranes. J Phys Chem B 113(13):4267–4274. doi:10.1021/jp805923k
21. van der Mynsbrugge J, Hemelsoet K, Vandichel M et al (2012) Efficient approach for the computational study of alcohol and nitrile adsorption in H-ZSM-5. J Phys Chem C 116(9):5499–5508. doi:10.1021/jp2123828
22. Svelle S, Tuma C, Rozanska X et al (2009) Quantum chemical modeling of zeolite-catalyzed methylation reactions: toward chemical accuracy for barriers. J Am Chem Soc 131(2):816–825. doi:10.1021/ja807695p
23. Greatbanks SP, Hillier IH, Burton NA et al (1996) Adsorption of water and methanol on zeolite Brønsted acid sites: an ab initio, embedded cluster study including electron correlation. J Chem Phys 105(9):3770. doi:10.1063/1.472197
24. Zhang J, Burke N, Yang Y (2012) Molecular simulation of propane adsorption in FAU zeolites. J Phys Chem C 116(17):9666–9674. doi:10.1021/jp301780z
25. Mallon EE, Babineau IJ, Kranz JI et al (2011) Correlations for adsorption of oxygenates onto zeolites from aqueous solutions. J Phys Chem B 115(39):11431–11438. doi:10.1021/jp208143t
26. Güvenç E, Ahunbay MG (2012) Adsorption of methyl tertiary butyl ether and trichloroethylene in MFI-type zeolites. J Phys Chem C 116(41):21836–21843. doi:10.1021/jp3067052
27. Lee C, Gorte RJ, Farneth WE (1997) Calorimetric study of alcohol and nitrile adsorption complexes in H-ZSM-5. J Phys Chem B 101(19):3811–3817. doi:10.1021/jp970711s
28. Mallon EE, Bhan A, Tsapatsis M (2010) Driving forces for adsorption of polyols onto zeolites from aqueous solutions. J Phys Chem B 114(5):1939–1945. doi:10.1021/jp910543r
29. van Speybroeck V, van der Mynsbrugge J, Vandichel M et al (2011) First principle kinetic studies of zeolite-catalyzed methylation reactions. J Am Chem Soc 133(4):888–899. doi:10.1021/ja1073992
30. Tuma C, Sauer J (2006) Treating dispersion effects in extended systems by hybrid MP2:DFT calculations-protonation of isobutene in zeolite ferrierite. Phys Chem Chem Phys 8(34):3955. doi:10.1039/b608262a
31. Kerber T, Sierka M, Sauer J (2008) Application of semiempirical long-range dispersion corrections to periodic systems in density functional theory. J Comput Chem 29(13):2088–2097. doi:10.1002/jcc.21069
32. Goltl F, Gruneis A, BuCko T et al (2012) Van der Waals interactions between hydrocarbon molecules and zeolites: periodic calculations at different levels of theory, from density functional theory to the random phase approximation and Møller–Plesset perturbation theory. J Chem Phys 137(11):114111–114117
33. Grimme S (2006) Semiempirical GGA-type density functional constructed with a long-range dispersion correction. J Comput Chem 27(15):1787–1799
34. Tkatchenko A, Scheffler M (2009) Accurate molecular van der Waals interactions from ground-state electron density and free-atom reference data. Phys. Rev. Lett 102(7):073005. doi: 10.1103/PhysRevLett.102.073005
35. Klimeš J, Bowler DR, Michaelides A (2010) Chemical accuracy for the van der Waals density functional. J Phys Condens Matter 22(2):22201
36. Dion M, Rydberg H, Schröder E et al (2004) Van der Waals density functional for general geometries. Phys Rev Lett 92(24):246401
37. Nabok D, Puschnig P, Ambrosch-Draxl C (2011) noloco: An efficient implementation of van der Waals density functionals based on a Monte-Carlo integration technique. Comput Phys Commun 182(8):1657–1662. doi:10.1016/j.cpc.2011.04.015
38. Kotrla J, Nachtigallová D, Kubelková L et al (1998) Hydrogen bonding of methanol with bridged OH groups of zeolites: ab initio calculation, ^{1}H NMR and FTIR studies. J Phys Chem B 102(14):2454–2463. doi:10.1021/jp9718055
39. Haase F, Sauer J (1994) ^{1}H NMR chemical shifts of ammonia, methanol, and water molecules interacting with Broensted acid sites of zeolite catalysts: ab-initio calculations. J Phys Chem 98(12):3083–3085. doi:10.1021/j100063a006
40. Haase F, Sauer J (1995) Interaction of methanol with Broensted acid sites of zeolite catalysts: an ab initio study. J Am Chem Soc 117(13):3780–3789. doi:10.1021/ja00118a014
41. Haase F, Sauer J, Hutter J (1997) Ab initio molecular dynamics simulation of methanol adsorbed in chabazite. Chem Phys Lett 266(3–4):397–402
42. Izmailova SG, Karetina IV, Khvoshchev SS et al (1994) Calorimetric and IR-spectroscopic study of methanol adsorption on zeolites. J Colloid Interface Sci 165(2):318–324. doi:10.1006/jcis.1994.1235
43. Krossner M, Sauer J (1996) Interaction of water with Brønsted acidic sites of zeolite catalysts. Ab initio study of 1:1 and 2:1 surface complexes. J Phys Chem 100(15):6199–6211. doi:10.1021/jp952775d
44. Vener MV, Rozanska X, Sauer J (2009) Protonation of water clusters in the cavities of acidic zeolites: $(H_2O)n \cdot$H–chabazite, $n = 1$–4. Phys Chem Chem Phys 11(11):1702. doi:10.1039/b817905k
45. Blaszkowski SR, van Santen RA (1995) Density functional theory calculations of the activation of methanol by a Broensted zeolitic proton. J Phys Chem 99(30):11728–11738. doi:10.1021/j100030a017
46. Gale JD, Catlow CRA, Carruthers JR (1993) An ab initio study of methanol adsorption in zeolites. Chem Phys Lett 216(1–2):155–161
47. Govind N, Andzelm J, Reindel K et al (2002) Zeolite-catalyzed hydrocarbon formation from methanol: density functional simulations. Int J Mol Sci 3(4):423–434. doi:10.3390/i3040423
48. Stich I, Gale JD, Terakura K, Payne MC (1998) Dynamical observation of the catalytic activation of methanol in zeolites. Chem Phys Lett 283(5–6):402–408
49. Broach RW, Jan D, Lesch DA, Kulprathipanja S, Roland E, Kleinschmit P (2013) Zeolites. Ullmann's Encycl Ind Chem (in press). doi:10.1002/14356007.a28_475.pub2
50. Bowen TC, Noble RD, Falconer JL (2004) Fundamentals and applications of pervaporation through zeolite membranes. J Membr Sci 245(1–2):1–33
51. Fujita H, Kanougi T, Atoguchi T (2006) Distribution of Brønsted acid sites on beta zeolite H-BEA: a periodic density functional theory calculation. Appl Catal A Gen 313(2):160–166. doi:10.1016/j.apcata.2006.07.017
52. Flanigen EM, Broach RW, Wilson ST (2010) Introduction. In: Kulprathipanja S (ed) Zeolites in industrial separation and catalysis. Wiley-VCH, Weinheim, pp 1–26
53. Wiesenborn DP, Rudolph FB, Papoutsakis ET (1988) Thiolase from *Clostridium acetobutylicum* ATCC 824 and its role in the synthesis of acids and solvents. Appl Environ Microbiol 54(11):2717–2722

54. Choi S, Lee J, Jang Y et al (2012) Effects of nutritional enrichment on the production of acetone–butanol–ethanol (ABE) by *Clostridium acetobutylicum*. J Microbiol 50(6):1063–1066. doi:10.1007/s12275-012-2373-1
55. Setlhaku M, Brunberg S, Villa Edel A, Wichmann R (2012) Improvement in the bioreactor specific productivity by coupling continuous reactor with repeated fed-batch reactor for acetone–butanol–ethanol production. Res Ind Biot CLIB-Graduate Cluster Pt II 161(2):147–152. doi: 10.1016/j.jbiotec.2012.04.004
56. Delley B (1990) An all-electron numerical method for solving the local density functional for polyatomic molecules. J Chem Phys 92(1):508. doi:10.1063/1.458452
57. Delley B (2000) From molecules to solids with the DMol^3 approach. J Chem Phys 113(18):7756. doi:10.1063/1.1316015
58. Accelrys, Inc. (2011) Materials Studio 6.0. Accelrys, Inc., San Diego. http://www.accelrys.com
59. Perdew JP, Burke K, Ernzerhof M (1996) Generalized gradient approximation made simple. Phys Rev Lett 77(18):3865–3868
60. Perdew JP, Burke K, Wang Y (1996) Generalized gradient approximation for the exchange-correlation hole of a many-electron system. Phys Rev B 54(23):16533–16539
61. Hansen N (2010) Multiscale modeling of reaction and diffusion in zeolites. Technische Universität Hamburg-Harburg, Hamburg
62. Hirshfeld FL (1977) Bonded-atom fragments for describing molecular charge densities. Theor Chim Acta 44(2):129–138. doi:10.1007/BF00549096
63. Mulliken RS (1955) Electronic population analysis on LCAO–MO molecular wave functions. I. J Chem Phys 23(10):1833
64. Mayer I (2007) Bond order and valence indices: a personal account. J Comput Chem 28(1):204–221. doi:10.1002/jcc.20494
65. Doronina LA, Izmailova SG, Karetina IV et al (1995) Calorimetric and IR-spectroscopic study of adsorption of methanol on zeolite-like aluminophosphates. Russ Chem Bull 44(10):1857–1862. doi:10.1007/BF00707212
66. Mirth G, Lercher JA, Anderson MW et al (1990) Adsorption complexes of methanol on zeolite ZSM-5. Faraday Trans 86(17):3039. doi:10.1039/ft9908603039
67. Kondo JN, Ito K, Yoda E et al (2005) An ethoxy intermediate in ethanol dehydration on Brønsted acid sites in zeolite. J Phys Chem B 109(21):10969–10972. doi:10.1021/jp050721q
68. Makarova MA, Williams C, Zamaraev KI et al (1994) Mechanistic study of *sec*-butyl alcohol dehydration on zeolite H-ZSM-5 and amorphous aluminosilicate. J Chem Soc Faraday Trans 90(14):2147–2153. doi:10.1039/FT9949002147
69. Pelmenschikov AG, van Wolput JHMC, Jaenchen J et al (1995) (A, B, C) triplet of infrared OH bands of zeolitic H-complexes. J Phys Chem 99(11):3612–3617. doi:10.1021/j100011a031
70. Catlow CRA, van Santen RA, Smit BJ (2004) Computer modelling of microporous materials, 1st edn. Elsevier, Amsterdam
71. Mihaleva VV, van Santen RA, Jansen APJ (2003) The heterogeneity of the hydroxyl groups in chabazite. J Chem Phys 119(24):13053. doi:10.1063/1.1628221
72. Limtrakul J, Tantanak D (1995) Structures, energetics and vibrational frequencies of zeolitic catalysts: a comparison between density functional and post-Hartree–Fock approaches. J Mol Struct THEOCHEM 358(1–3):179–193
73. Payne MC, Hytha M, Štich I et al (2001) First principles calculation of the free energy barrier for the reaction of methanol in a zeolite catalyst. Microporous Mesoporous Mater 48(1–3):375–381
74. Rimola A, Costa D, Sodupe M et al (2013) Silica surface features and their role in the adsorption of biomolecules: computational modeling and experiments. Chem Rev 113(6):4216–4313. doi:10.1021/cr3003054
75. Kongpatpanich K, Nanok T, Boekfa B et al (2011) Structures and reaction mechanisms of glycerol dehydration over H-ZSM-5 zeolite: a density functional theory study. Phys Chem Chem Phys 13(14):6462. doi:10.1039/c0cp01720e
76. Datt A, Fields D, Larsen SC (2012) An experimental and computational study of the loading and release of aspirin from zeolite HY. J Phys Chem C 116(40):21382–21390. doi:10.1021/jp3067266
77. Boekfa B, Sirijareansre J, Limtrakul P, Pantu P, Limtrakul J (2007) Adsorption of glycine amino acid in zeolite: an embedded QM/MM study. Proc NSTI-Nanotech 1:454–457
78. Plant DF, Simperler A, Bell RG (2006) Adsorption of methanol on zeolites X and Y. An atomistic and quantum chemical study. J Phys Chem B 110(12):6170–6178. doi:10.1021/jp0564142
79. Shah R, Gale JD, Payne MC (1996) Methanol adsorption in zeolites: a first-principles study. J Phys Chem 100(28):11688–11697. doi:10.1021/jp960365z
80. Milestone NB, Bibby DM (1981) Concentration of alcohols by adsorption on silicalite. J Chem Technol Biotechnol 31(1):732–736
81. García-Serrano LA, Flores-Sandoval CA, Zaragoza IP (2003) Theoretical study of the adsorption of isobutane over H-mordenite zeolite by ab initio and DFT methods. J Mol Catal A Chem 200(1–2):205–212. doi:10.1016/S1381-1169(02)00680-5
82. Bolis V, Busco C, Ugliengo P (2006) Thermodynamic study of water adsorption in high-silica zeolites. J Phys Chem B 110(30):14849–14859. doi:10.1021/jp061078q